catalysts

MDPI

Article

Photocatalytic Selective Oxidation of Ammonia in a Semi-Batch Reactor: Unravelling the Effect of Reaction Conditions and Metal Co-Catalysts

Elnaz Bahadori [1], Francesco Conte [2], Antonio Tripodi [2], Gianguido Ramis [1] and Ilenia Rossetti [2,*]

[1] Dip. Ing. Chimica, Civile ed Ambientale, Università degli Studi di Genova and INSTM Unit Genova, via all'Opera Pia 15A, 16145 Genoa, Italy; elbaha65@gmail.com (E.B.); gianguidoramis@unige.it (G.R.)
[2] Chemical Plants and Industrial Chemistry Group, Dip. Chimica, Università degli Studi di Milano, CNR-ISTM and INSTM Unit Milano-Università, via C. Golgi 19, 20133 Milan, Italy; francesco.conte@unimi.it (F.C.); antonio.tripodi@unimi.it (A.T.)
* Correspondence: ilenia.rossetti@unimi.it; Fax: +39-0250314300

Abstract: Photocatalysis has been used for the oxidation of ammonia/ammonium in water. A semibatch photoreactor was developed for this purpose, and nanostructured TiO_2-based materials, either commercial P25 or prepared by flame spray pyrolysis (FSP), were used as catalysts. In the present work, we investigated the effect of (i) metal co-catalysts, (ii) pH, and (iii) ammonia concentration on the efficiency of oxidation and on the selectivity to the undesired overoxidation byproduct, i.e., nitrites and nitrates. Several metals were added to both titania samples, and the physicochemical properties of every sample were studied by XRD, BET, and UV-Vis spectroscopy. The pH, which was investigated in the range of 2.5–11.5, was the most important parameter. The optimum pH values, resulted as 11.5 and 4.8 for P25 and FSP respectively, matching the best compromise between an acceptable conversion and a limited selectivity toward nitrite and nitrate formation. For both titania samples (P25 and FSP), ammonia conversion vs. nitrite and nitrate formation were highly dependent on the pH. At pH $\geq$ 9, the initial rate of photooxidation was high, with selective formation of overoxidized byproducts, whereas, at a more acidic pH, the conversion was lower, but the selectivity toward nitrogen formation was higher. P25 samples added with noble metal co-catalysts (0.1 mol% Ag, Au, Pd, Pt) at pH = 11.5 remarkably increased the selectivity to nitrite and nitrate, while, in the case of FSP samples (pH = 4.8), the co-catalysts increased the selectivity toward N_2 with respect to the unpromoted catalyst and also the conversion in the case of Au and Pt. Reactivity was discussed, leading to the proposing of a mechanism that correlates the activity with either surface adsorption (depending of the surface charge of the catalyst and on pH) or the homogeneous reactivity of oxidizing species.

Keywords: ammonia photocatalytic oxidation; photocatalysis; photocatalysts; wastewater treatment; advanced oxidation processes (AOPs)

Citation: Bahadori, E.; Conte, F.; Tripodi, A.; Ramis, G.; Rossetti, I. Photocatalytic Selective Oxidation of Ammonia in a Semi-Batch Reactor: Unravelling the Effect of Reaction Conditions and Metal Co-Catalysts. *Catalysts* **2021**, *11*, 209. https://doi.org/10.3390/catal11020209

Academic Editor: Fernando J. Beltrán Novillo
Received: 5 January 2021
Accepted: 1 February 2021
Published: 5 February 2021

1. Introduction

Aqueous ammonia (NH_3) is one of the major nitrogen-containing pollutants in wastewater and is a potential source of oxygen depletion due to eutrophication [1–4]. Both ammonium (NH_4^+, pKa = 9.3 at 25 °C [5]) and its conjugate base (NH_3) can be present in water and wastewater. The toxicity is commonly attributed only to NH_3 and not to NH_4^+; nevertheless, the equilibrium partition in water of the two species depends on pH, temperature, and ionic strength. Therefore, NH_4^+ can exist in natural water while NH_3 can reach toxic levels in alkaline water.

Ammonia can be produced through natural sources, such as gas exchange with the atmosphere, chemical and biochemical degradation of N-containing substances, and the excretion by biota [6]. Commercially, NH_3 is synthesized by the so-called Haber–Bosch

process [7,8], which is extensively used as a basis for the production of a vast variety of chemicals, such as fertilizers, explosives, nitric acid, and polyamides. This represents a method for the fixation, i.e., activation of atmospheric nitrogen, and considering that 85% of 146 million ton per year of the ammonia produced worldwide is used for fertilizers production [8], one may appreciate the magnitude of admission of this nutrient in the environment, particularly in surface or ground waters.

Several methods are used for NH_4^+/NH_3 removal from water and wastewater, including ammonia stripping, biological nitrification, ion exchange, and breakpoint chlorination, but each one has drawbacks [1]. For instance, temperature, pH, dissolved oxygen, carbon source, and the concentrations of toxic substances have direct impact on the efficiency of biological nitrification [9,10]. Breakpoint chlorination may produce harmful byproducts and requires further treatments for residuals [11]; consequently, it may produce highly concentrated wastes, which is even more difficult to treat.

Several studies have been performed recently to find a selective and environmentally friendly method for the one-pot abatement of N-containing pollutants. In this regard, photocatalytic oxidation of NH_4^+/NH_3 has been investigated, and different catalysts were studied in recent years [12–17]. It was demonstrated that solar radiation can be used in photocatalysis, which would make it economically competitive for water and wastewater treatment [18]. While some studies investigate the effect of pH on reactivity and selectivity of the NH_4^+/NH_3 photooxidation [15,19–21], no affordable report is available for explaining this trend. Bravo et al. [15] proposed that the electrostatic properties of catalysts surface in different environments with the reactive compounds plays an important role on the rate of the reaction. However, Bonsen et al. [21] proposed that at basic pH (pH > 9.3), the scenario is different and the adsorption of neutral NH_3, rather than NH_4^+ on the surface of TiO_2, may be the rate-limiting step. Thus, a clear conclusion on the effect of pH is not available yet and depends on the adsorption properties of the catalyst.

On the other hand, one of the main efficiency issues in photocatalytic processes is the fast electron-hole recombination (~10^{-9} s). In order to overcome this problem, semiconductors are often loaded with noble metal nanoparticles [22–24]. These nanoparticles have the Fermi level located near the energy potential of the semiconductor conduction band, and therefore they are able to capture photopromoted electrons. The addition of some noble metals (e.g., Au) may also improve the light harvesting through the plasmonic effect. Furthermore, if metal addition is followed by thermal reduction in H_2 to reduce the metal, as reported, e.g., in [25], the presence of the metal itself can favor titania reduction during the activation in reducing environment, thus indirectly decreasing the titania band gap.

Previously, we considered the effect of titania samples promoted with different co-catalysts for application in a photoreduction reaction, i.e., the photoreduction of nitrate in water, exploring the potential of different catalyst formulations and of reaction conditions. In this work, we focus instead on the use of the same catalysts as mediators for the oxidation of a pollutant in water. To this purpose, we set up a semibatch reactor for the photooxidation of ammonia, where ammonia-containing water is fed to the reactor at the beginning of the reaction, while oxygen or air is fed continuously to the reactor. Water soluble byproducts (NO_3^- and NO_2^- due to ammonia overoxidation) are accumulated simultaneously into the reactor, whereas molecular N_2, the desired product of selective oxidation, is withdrawn continuously from the reactor.

The aim of current study is to investigate the mechanism, conversion and selectivity of different photocatalysts for the photooxidation of NH_4^+/NH_3. For this purpose, the optimum pH conditions are selected over a commercial TiO_2 sample (Evonik P25) and a similar nanostructured TiO_2 obtained by a home-developed apparatus for Flame Spray Pyrolysis (FSP). The latter technique, applied to different materials and processes, is proven able to produce materials with significantly higher surface concentration of hydroxyl groups, in turn affecting surface properties [26–28]. Based on the optimum pH, the conversion and the selectivity toward different products of photocatalysts, either as such or with different

metal co-catalysts (0.1 mol% Ag, Au, Pd and Pt, loaded by impregnation on both titania samples), are investigated.

2. Results and Discussion

The catalysts used in this work are based on nanostructured TiO_2 prepared by two different flame-based methods, namely flame hydrolysis of a volatile chloride precursor (the well-known TiO_2 P25 Aeroxide®) and flame spray pyrolysis (FSP). Although leading to similar physical chemical properties (see Table S1), the residence time and temperature of the flame are different [29], possibly leading to different porosity and crystal phases ratio. The catalysts were used as such or added with different noble metal co-catalysts (0.1 mol% Ag, Au, Pt or Pd). These catalysts were extensively characterized in a previous work and tested for their photoreductive properties [25]. Here, the activity and selectivity for the photooxidation of ammonia are instead being tested.

The main features of the catalyst can be found in the cited reference and are summarized in the Supporting Information (SI) file. Briefly, the XRD analysis evidenced the same crystalline structure for every sample, which is composed of a mixture of anatase and rutile phases of TiO_2 in different proportions, and the FSP samples showed a slightly higher surface area, rutile content, and bigger crystal size than P25.

All the materials showed a strong absorption in the range of 240–380 nm, but for pure TiO_2 samples, the calculated band-gap was higher with respect to the metal-added ones. Only in some cases, some plasmon resonance was observed (e.g., with Au).

2.1. Activity Testing for Photooxidation of Ammonia

The photocatalytic activity data were elaborated through a model assuming consecutive first-order transformation of NH_4^+/NH_3 to N_2 then consecutively to NO_2^- and further to NO_3^- [30]. No product different from N_2, NO_3^- and NO_2^- was detected. According to the possible intermediates and based on kinetic investigations, the mechanism can be described as depicted in Scheme 1. For 1 g/L of TiO_2 concentration, the rate constants for NO_2^- photocatalytic oxidation to NO_3^- were by far more dependent on TiO_2 concentration than those for NH_4^+/NH_3 oxidation to NO_2^-, signifying the role of sufficient TiO_2 concentration for initiating the overoxidation of NH_4^+/NH_3 to NO_3^- [30].

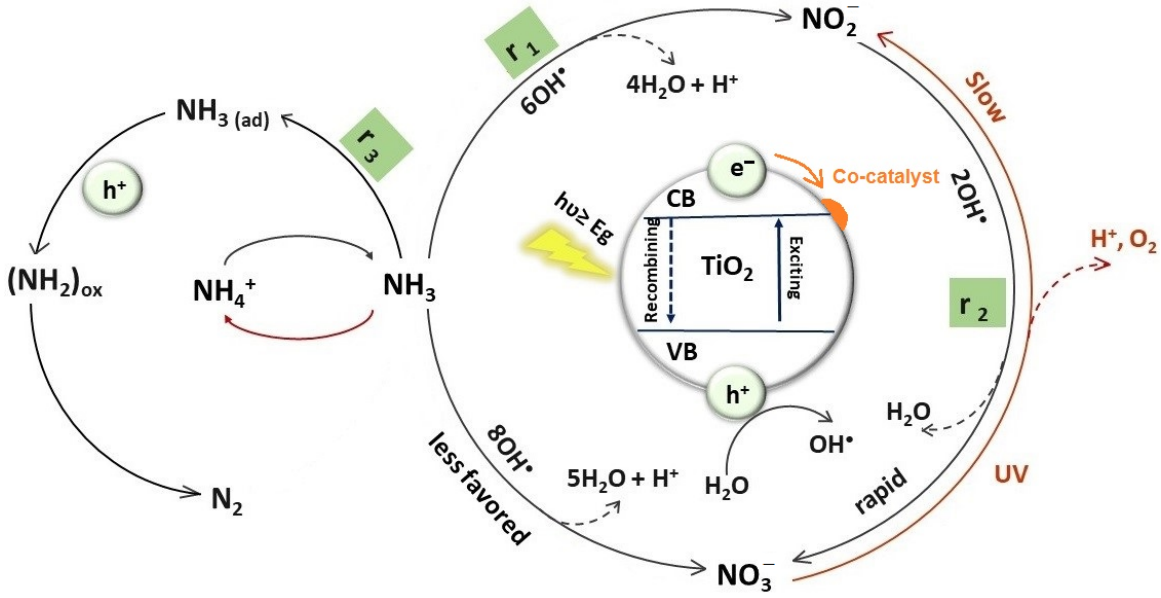

Scheme 1. Mechanism of photooxidation of NH_4^+/NH_3 with different reaction pathways. Scheme readapted from [17].

2.1.1. Effect of Ammonia Concentration

The photocatalytic tests were performed on the P25 sample with three different ammonia concentrations (0.012, 0.02 and 0.2 M) at pH 5.1. This pH corresponds to a 0.2 M solution of NH_4Cl dissolved in bi-distilled water, without any adjustment.

According to Figure 1, initial photooxidation rates were proportional to the initial concentration of NH_3, as evidenced recently also by Ren et al. [16]. Since at this pH value the catalysts' surface was nearly neutral, by increasing the initial ammonia concentration from 0.012 up to 0.2 M, more NH_3 adsorbed on the catalysts' surface, and consequently the rate of photooxidation increased up to ten times. Meanwhile, NO_3^- selectivity decreased from 3.7% to 0%.

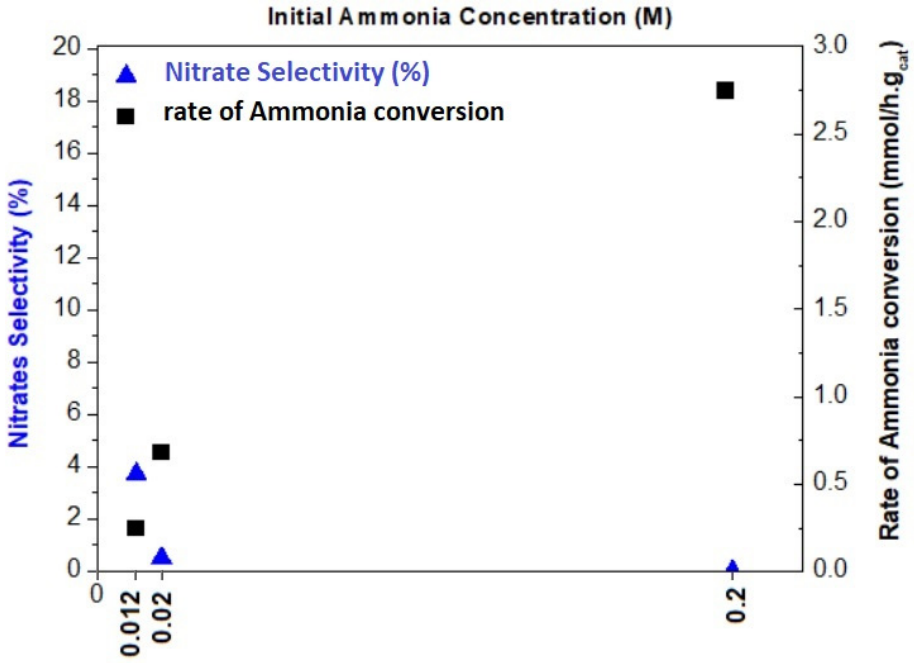

Figure 1. Rate of ammonia conversion and nitrate selectivity for the P25 sample at three different initial concentration of ammonia and constant pH of 5.1.

Electrostatically driven adsorption may increase the surface concentration of the reactant at variable pH, and it is important to note that the initial concentration of NH_3 (neutral form) showed to be a predominant factor in improving the reaction rate with respect to the total concentration ($[NH_4^+] + [NH_3]$). According to previous studies [31,32], the reaction rate between neutral NH_3 and $OH^\bullet$ at 25 °C was much higher than that between NH_4^+ and OH. Thus, the pH-dependent equilibrium between NH_4^+ and NH_3, and not the pH-dependent electrostatic attraction between NH_4^+ and the TiO_2 surface, which will be discussed later in this work, plays a key role in the photooxidation reaction.

Here, 0.2 M was selected as the initial concentration of ammonia for the further experiments, which represent the case of a highly concentrated industrial wastewater.

As seen in Scheme 1, $(NH_2)_{ox} = NH_2OH$ or H_2NNH_2, as deduced from literature data [30].

2.1.2. Effect of pH

The effect of pH for different photocatalysts was investigated using a solution of HCl or NaOH to tune the pH of the native NH_4Cl solution. The selected pH values were 2.5, 4.8, 5.1, 9.0, and 11.5. As mentioned, a pH value of 5.1 was obtained with a 0.2 M solution of NH_4Cl and bi-distilled water.

An example of the time dependence of conversion and selectivity for both bare titania samples at pH = 9.11 is reported in Figure 2.

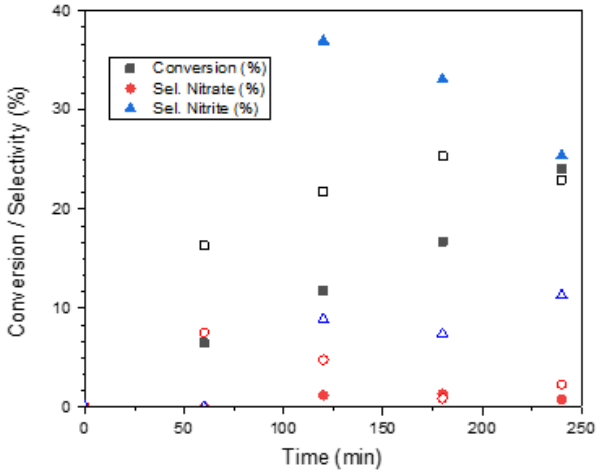

Figure 2. Time dependence of conversion and selectivity. Full symbols = sample P25, hollow symbols sample FSP.

As expected, the ammonia conversion increased with reaction time. The activity of the FSP titania was higher than that of the P25 sample, with generally lower selectivity to nitrite and nitrate. Some reversibility of the reaction can be also hypothesized, since the same catalysts can be active also for the photoreduction of nitrite and nitrate as recently demonstrated [25].

The pH level not has only an important role in assessing the equilibrium between NH_4^+ and NH_3, but it also drives the surface interaction with the photocatalyst. Electrostatically favored adsorption may improve the rate of ammonia photooxidation by increasing its surface concentration. To account for this, it is important to understand the surface charge status of the sample. For instance, in pH ranges lower than the point of zero charge (PZC) of the semiconductor, the surface is positively charged, and this should not favor the adsorption of ammonium (species present at such a low pH) over the surface. By contrast, at pH higher than PZC, the surface should be negatively charged, favoring ammonium adsorption. At even higher pH, ammonium deprotonates to neutral ammonia, thus leading to the adsorption of the neutral species over the negatively charged surface. Therefore, if the rate-determining step of the reaction would be the surface adsorption, we should expect a higher rate in the pH range between the PZC and pKa of ammonia (negative surface + positively charged reactant).

The surface charge status of P25 and FSP catalysts was firstly studied, basing on the electrophoretic mobility as a function of pH at 25 °C through the electrophoretic light scattering technique. Consequently, the point of zero charge (PZC) was obtained based on ζ potential measurements as pH 6.25 and 4.5 for P25 and FSP, respectively (Figure 3a). Different pH values correspond to nil charge for the two different titania samples: ca. 4.5 for FSP and ca. 6.5 for P25.

The particle size distribution and agglomeration may also be affected by surface charge, and it was studied by means of the dynamic light scattering (DLS) technique (Figure 3b). Indeed, neutral nanoparticles may tend to agglomerate easier than surface charged ones. According to Figure 3b, P25 showed more uniform size with varying pH, while higher coagulation was observed for FSP particles at basic pH, with consequent possible modification of surface exposure.

Electrostatic-based adsorption can help to comparatively describe the pH dependence on reactions pathway and the initial rates of intermediates formation for both P25 and FSP photocatalysts. Milis and Doménech [33] suggested that, as for NH_4^+, the electrostatic interaction between possibly charged intermediates, such as NO_2^- and the TiO_2 surface, affects the reaction rate of the further NO_2^- oxidation to NO_3^- and consequently the reaction selectivity pattern, besides the conversion of ammonia, at different pH values.

Therefore, it is important to understand which reaction is the rate-limiting step in the oxidation of NH_4^+/NH_3.

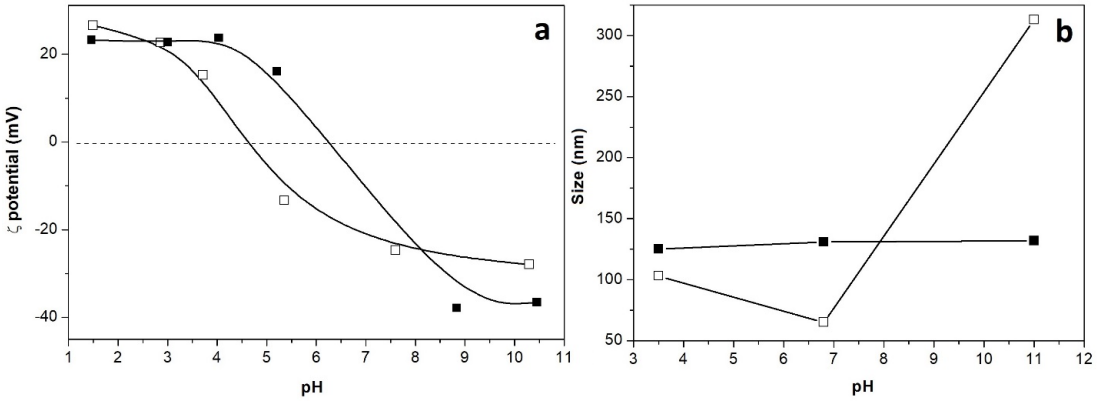

Figure 3. (**a**) ζ−potential curves (reproduced from [25] by kind permission of John Wiley and Sons) and (**b**) size of the particles in the solution based on dynamic light scattering (DLS) behavior at different pH. P25 shown as full squares, FSP as hollow squares.

The conversion of ammonia and the relative selectivity to byproducts is reported after 120 min of reaction for the FSP sample and 240 min for P25 (time at which the maximum conversion was achieved, respectively). The selectivity to N_2 can be roughly deduced as complement to 100% with respect to the selectivities to nitrate and nitrite. Indeed, N_2 was monitored through gas chromatography, but the selectivity to N_2 cannot be calculated in a comparable way with respect to that of nitrite and nitrate with the current experimental set up. Indeed, ammonia, nitrite and nitrate accumulate in the photoreactor, and their concentration is monitored every hour through liquid sampling. By contrast, due to the semibatch reactor configuration, with continuous gas flowing, N_2 is not allowed to accumulate for 1 h and to be sampled to provide the same selectivity data. Its measure allowed us to calculate the overall N-balance throughout the whole test, which closed between 95% and 110%, depending on the conditions.

At pH = 2.5, ammonia conversion of about 11% (after 4 h reaction time) and 26% (after 2 h reaction time) was obtained for bare P25 and FSP, respectively (Figure 4). No trace of NO_2^- was observed for both catalysts, and there was only a small selectivity to nitrate. In this range of pH ($pH \leq pH_{PZC}$), both catalysts have a positively charged surface, which should hinder the electrostatic adsorption of NH_4^+. At this pH, both photocatalysts are mainly selective to N_2 production (r3 in Scheme 1).

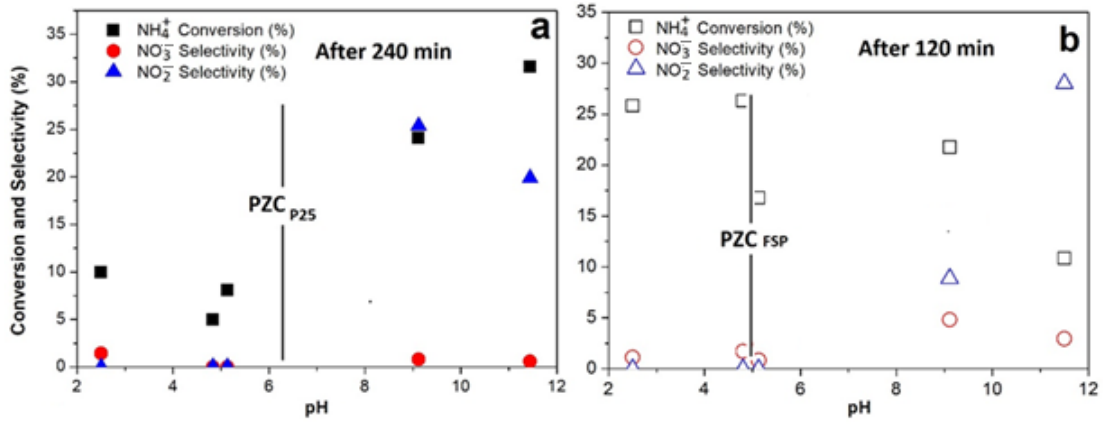

Figure 4. Conversion of NH_4^+/NH_3 and NO_2^- and NO_3^- selectivity vs. pH considering the sample (**a**) after 240 min of reaction for P25 (solid colored symbols); (**b**) after 120 min for FSP (hollow symbols). Conversion and selectivity (%) figures on y-axis of diagrams (**a**,**b**).

In the range 2.5 ≤ pH ≤ 5.1, the ammonia conversion and selectivity did not change appreciably (Figure 4). This range of pH is still below the pH_{pzc} of P25, at which the net surface charge would be neutral, with a very moderate agglomeration of the particles (Figure 3b). According to Letterman [34], this phenomena can result in the variation and reduction in the surface area and finally to a slower rate of the surface reactions, in any case limited. However, Butler et al. [30] proposed that coagulation/flocculation does not play a major role on reaction rates with respect to the effect of other parameters, which is in agreement with the results of our experiments on FSP catalysts (Figure 4b), where widely different coagulation occurred (Figure 3b), but with limited effect on conversion.

At pH values below the pKa of NH_4^+ ($pK_{a\ (NH_4)}$ = 9.2 at 25 °C), ammonium is the predominant species, transforming into neutral ammonia at higher pH. Meanwhile, at pH lower than PZC the surface is positively charged, while at pH > PZC it is negatively charged. Based on the PZC of the two catalysts, which is different, ammonium should adsorb over a positive surface until neutral pH for P25, over a negative surface between 6.5 and 9.2, while at higher pH the ammonia should interact as a neutral molecule over a negatively charged surface. On the contrary, for FSP the range in which a negative surface can host the positive ammonium ion is extended at pH = 4.5–9.2. This can explain the different reactivity moving through the PZC of each catalyst, considering the contribution of surface adsorption of ammonia/ammonium. A similar increase of conversion with increasing pH was observed by Shibuya et al. [35].

Indeed, from 5 ≤ pH ≤ 9, the rate of photooxidation of NH_4^+/NH_3 increased fairly steeply, but together with increasing selectivity to NO_2^- for both P25 and FSP (Figures 4 and 5). When the $pH_{pzc} \leq pH \leq pK_{a\ (NH_4^+)}$ ($pK_{a\ (NH_4^+)}$ = 9.2 calculated from the standard Gibbs energy at 25 °C), the negatively charged surface of TiO_2 may favor the adsorption of NH_4^+. Therefore, if surface adsorption is the rate-determining factor, the highest reaction rates would be expected in this pH region, which is not the case. Indeed, the further increase of the rate of ammonia oxidation for pH higher than 9 indicates that electrostatically favored adsorption is not the rate-limiting step (Figure 5). Considering the negatively charged surface of both TiO_2 samples at high pH (9 and 11.5) and simultaneously the higher fraction of NH_3 with respect to NH_4^+ at pH 11.5 than 9, it is suggested that for both P25 and FSP photocatalysts, the photooxidation of ammonia should be preferentially mediated by oxidizing radicals OH, as recently discussed [25].

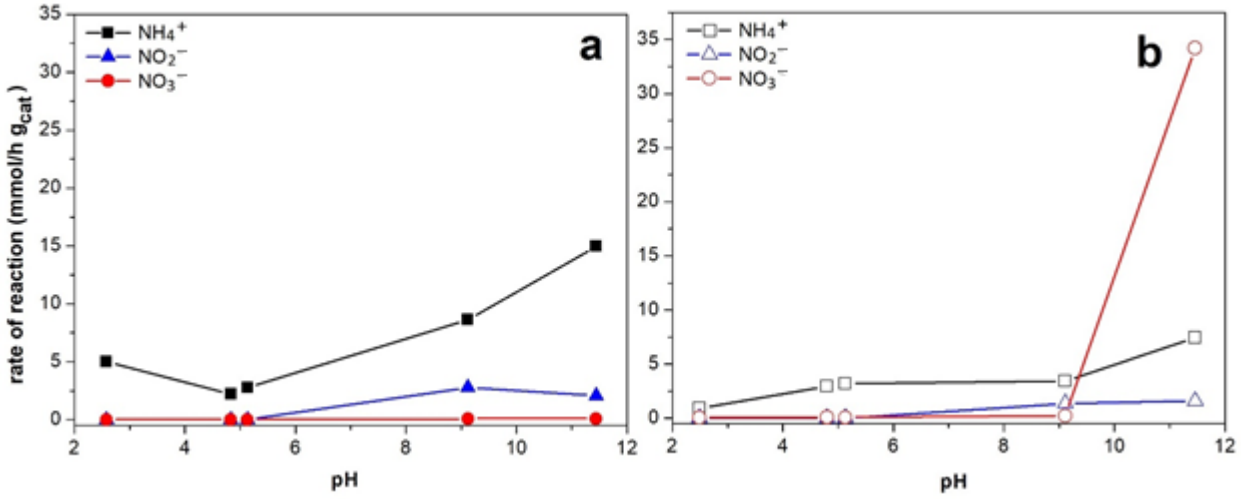

Figure 5. Rate of NH_4^+/NH_3 oxidation and of NO_2^- and NO_3^- production vs. pH, considering the data after 5 h of reaction for (**a**) P25 (solid colored symbols) and (**b**) FSP (hollow symbols). Rate of reaction figures on y-axis of diagrams (**a**,**b**).

The different selectivity pattern can be instead correlated to the dependence on pH of the redox potentials of the species involved [25].

This behavior was observed also in some other studies [30,36–39]. According to Butler et al. [30], the rate constant of the reaction between neutral NH_3 and $OH^\bullet$ was $1 \times 10^8 \left(\frac{1}{M\ s}\right)$ (25 °C), comparing to very slow reaction rate (almost impossible to measure) between NH_4^+ and $OH^\bullet$. Consequently, the higher reactivity of electrophilic $OH^\bullet$ with neutral NH_3 with respect to NH_4^+ may explain the higher initial rates at pH 11.5 than at pH 9.0 (Figure 5).

Also the NO_2^- and NO_3^- formation rates were found to be highly dependent on pH (Figure 4). When the initial pH was higher than 9, the photooxidation of NH_4^+/NH_3 resulted in the formation of NO_2^- and NO_3^-. This unselective oxidation was also observed in different studies with UV-irradiated TiO_2 [17,20,40], in which NO_2^- was either the product of photooxidation of NH_4^+/NH_3 or photoreduction of NO_3^-. This is in line with a homogeneous type reactivity with respect to a surface-mediated one: The catalyst predominantly acts as generator of activated oxidizing radicals, which then react unselectively in the liquid phase.

As a result, in combining the activity for ammonia photooxidation and selectivity to overoxidation products, the pH levels 11.5 and 4.8 were selected as optimum pH values for P25 and FSP, respectively. For FSP, this condition successfully corresponds to high conversion of ammonia and negligible selectivity to overoxidized byproducts, while for P25 it represents a satisfactory compromise between high conversion and acceptable selectivity to byproducts.

A similar conversion trend vs. pH but a much lower selectivity to overoxidized byproducts at basic pH was obtained here with bare P25 with respect to literature data [41], while the FSP sample allowed us to overperform literature data at acidic and nearly neutral pH.

2.1.3. Effect of Co-Catalyst

The results of photooxidation tests with different co-catalysts at the optimum pH previously determined are plotted in Figure 6. Metal NPs dispersed on the semiconductor, with suitable function, can act as electron traps ensuring better separation of the photoproduced charges and consequently higher rates of hole-mediated oxidation reactions. For a potential use under solar light irradiation, they may also improve light harvesting through plasmonic effect (e.g., Au).

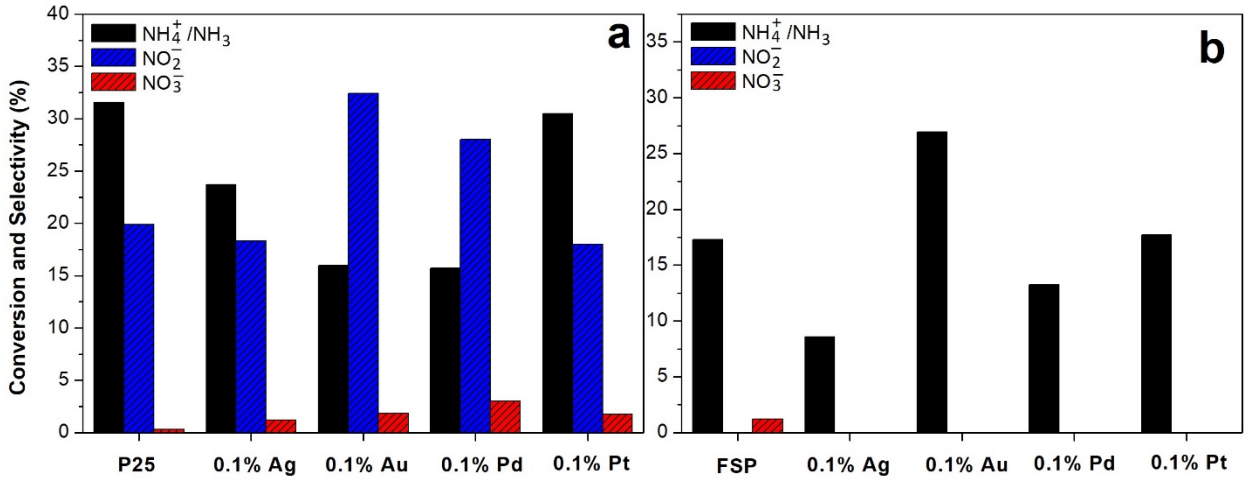

Figure 6. Ammonia conversion and NO_x^- selectivity after 240 min of irradiation with different co-catalysts on (**a**) P25 at pH 11.5 and (**b**) FSP at pH 4.8. Conversion and selectivity (%) figures on y-axis of diagrams (**a**,**b**).

Considering the P25-based photocatalysts at the selected pH of 11.5, the addition of metals depressed the conversion of NH_3 and also increased the selectivity to nitrite and nitrate anions. Thus, the unselective oxidation was favored, placing overall a higher number

of active oxidizing species, but failing the selectivity targets. Only Pt showed comparably active and selective than bare P25 but with higher cost of the material (Figure 6a). Similarly, high selectivities to NO_x^- were obtained with Ag/P25 at basic pH by Ren et al. [16]. By contrast, with respect to these results, much higher activity was previously reported for Pt/P25 [42].

The results obtained on metal-added FSP samples at pH 4.8 (Figure 6b) show in every case nil selectivity for nitrites and nitrates, thus matching the selectivity goal. As in the case of P25 samples, Pt showed comparable ammonia conversion with respect to the unpromoted catalyst, while Au addition further improved the conversion.

The P25 and the FSP-based samples have similar phase composition, which is not particularly critical for this application. It is well known that a mixed phase for titania base materials helps the segregation of the photogenerated charges [43,44], so from this point of view, all the samples are almost identical. The specific surface area of every sample is of similar order of magnitude, with slightly higher values (10–15%) for the FSP samples than for the P25 ones. This factor can be important for improving the surface adsorption, provided that proper electrostatic interaction subsists. For instance, in the pH range where NH_4^+ adsorption may take place over the negatively charged surface (PZC < pH < pKa), a higher available surface means a higher concentration of the reactant. This may further explain the higher reactivity of the FSP sample at intermediate pH.

In addition, both the Au- and Pt-promoted photocatalysts were characterized by a lower band gap than the unpromoted sample, as detailed in SI, while the other physical chemical parameters were kept almost unaltered. This means that a higher population of electrons can overcome the band gap under the same irradiance. However, if the reactivity for photooxidation is predominantly mediated by $OH^\bullet$, these can be produced also through the transfer of an electron from the conduction band of titania to O_2, co-fed to the reactor, with formation of oxidizing species such as the superoxide $O_2^{-\cdot}$ and H_2O_2 and their further decomposition to $OH^\bullet$, according to Scheme 2. Thus, the role of the metal as an electron sink changes the reactivity (kinetics and thermodynamics) of the valence band electron, altering this pathway to the formation of the oxidizing species.

In other words, if the reactivity is predominantly due to the hole or electron from the semiconductor for forming oxidizing species acting in liquid phase (as at basic pH, through Reactions (4) or (5) in Scheme 2), there is no need to add a metal as an electron sink, since oxygen itself can react with the photopromoted electron (Reaction (5)) and OH^- with the holes (Reaction (4)) to form strongly oxidizing species. Thus, the addition of the metal co−catalyst can have negligible or even detrimental effect as in the case of the P25−based catalysts, tested under basic conditions.

By contrast, the FSP sample can be used with a reasonable conversion at pH values where higher selectivity to N_2 is achieved. Indeed, at neutral or acidic pH, the concentration of homogeneous radicals is lower (due to the suppression of Reaction (4) and the presence of alternative paths for the evolution of $O_2^{\cdot}$ through Reactions (6) and (7)), and thus the reactivity becomes slower than at basic pH, but also the unselective oxidation to nitrite and nitrate is limited. Thus, on one hand, it can be hypothesized that catalysts that are more effective in the direct activation of the substrate, directly transferring holes to the adsorbed ammonia, may be more active and selective when operating around neutral or slightly acidic pH. If this reaction route is not effective, for instance because the PZC is too high to guarantee a suitable pH range to have a negatively charged surface for ammonium adsorption, satisfactory activity can be achieved only at basic pH, where the homogeneous reaction between strongly oxidizing species and ammonia leads to higher activity, but also unselective overoxidation. On the other hand, at neutral/basic pH, the electron sink effect by some metals, which improves charge separation, may be more effective in improving the conversion, while keeping satisfactory the selectivity to N_2, as for the Au-promoted FSP catalyst.

$$TiO_2 + h\nu \xrightarrow{\lambda < 385\ nm} e^-_{cb} + h^+_{vb} \quad (1)$$

$$e^-_{cb} + h^+_{vb} \rightarrow heat \quad (2)$$

$$h^+_{vb} + H_2O \rightarrow \cdot OH + H^+ \quad (3)$$

$$h^+_{vb} + OH^- \rightarrow \cdot OH \quad (4)$$

$$e^-_{cb} + O_2 \rightarrow O_2^{\cdot -} \quad (5)$$

$$O_2^{\cdot -} + O_2^{\cdot -} + 2H^+ \rightarrow H_2O_2 + O_2 \quad (6)$$

$$O_2^{\cdot -} + H^+ \rightarrow HO_2^{\cdot} \quad (7)$$

$$e^-_{cb} + H^+ + HO_2^{\cdot} \rightarrow H_2O_2 \quad (8)$$

$$H_2O_2 + h\nu \rightarrow 2 \cdot OH \quad (9)$$

$$H_2O_2 + e^-_{cb} \rightarrow OH^- + \cdot OH \quad (10)$$

Scheme 2. Generation of oxidizing species over bare TiO_2.

Overall, the FSP titania catalyst allowed for reaching higher ammonia conversion at low pH, where the selectivity to undesired overoxidation byproducts formation is negligible. Satisfactory results can be achieved with the unpromoted sample at pH 4.8, which is further improved by the addition of a small amount of Au (0.1 mol%).

The results above reported can be compared with what was reported by Altomare et al. [45], who compared the effect of the same metals supported over P25 at pH = 10. Similar findings were achieved when testing the bare P25, except the lower selectivity to nitrate overall that was observed in the present work. The effect of metal addition was more pronounced in the cited literature, whereas it was negligible here, mostly due to the very low loading here selected. This, in turn, was chosen to limit the cost of the material, which is one of the main factors impacting the economic feasibility of the process.

3. Materials and Methods

3.1. Materials Preparation

TiO_2-FSP samples were obtained by means of a homemade apparatus [28,46], consisting of a burner through which a solution of the titania precursor and 5 L/min of oxygen are fed. A ring of flamelets (0.5 L/min CH_4 + 1 L/min of O_2) ignite and stabilize the flame.

The TiO_2 precursor (titanium isopropoxide, Sigma Aldrich − Merck Life Science S.r.l., Milan, Italy, pur. 97%) was dissolved in an organic solvent (o-xylene and propionic acid, 1:1 *v*/*v*, Sigma Aldrich − Merck Life Science S.r.l., Milan, Italy, pur. 97%) with a 0.4 M concentration and was constantly fed to the burner (2.5 mL/min) through a syringe pump. The pressure drop at the burner nozzle was set at 1.5 bar.

A sample of TiO_2 P25 supplied by Evonik (Hanau-Wolfgang, Germany) was used as a commercial benchmark, i.e., an example of flame-prepared nanosized material. The fine white powder was obtained by flame hydrolysis of $TiCl_4$ in a preformed H_2-O_2 flame.

Different metals were added as co-catalysts to both P25 and FSP TiO_2, using different metal precursors by impregnation and subsequent reduction by heating at 10 °C/min in H_2 flow at different temperatures for 3 h, according to preliminary temperature programmed reduction (TPR). In particular, we added the following, all supplied by Sigma Aldrich − Merck Life Science S.r.l., Milan, Italy:

- 0.1 mol% of Au, from $NaAuCl_4 \cdot 2H_2O$, T_{TPR}: 700 °C;
- 0.1 mol% of Ag, from $AgNO_3$, T_{TPR}: 150 °C;
- 0.1 mol% of Pd, from $Pd(NO_3)_2 \cdot xH_2O$, T_{TPR}: 300 °C;
- 0.1 mol% of Pt, from Pt(Acetylacetonate)$_2$, T_{TPR}: 700 °C.

3.2. Materials Characterization

X-ray diffraction (XRD) was done with a Philips 3020 (Philips, Eindhoven, Netherlands) apparatus using the Cu-Kα (λ = 1.5406 Å) radiation, with a graphite monochromator on the diffracted beam. Data span was in the 20°–90° 2θ range with 0.03° step size and 4 s step time. The voltage and current intensity of the generator were set at 40 kV and 30 mA, respectively.

N_2 adsorption and desorption experiments were carried out on a Micromeritics ASAP2020 (Norcross, GA, US) apparatus. BET SSA was calculated according to the Brunauer−Emmett−Teller model. Adsorption isotherms were collected at 77 K on samples previously outgassed at 150 °C overnight. Micropores volume was calculated with the t-plot method.

Diffuse reflectance (DR) UV−Vis spectra of samples were collected by means of a Cary 5000 UV-Vis-NIR spectrophotometer (Varian instruments, Palo Alto, CA, US) between 200 and 800 nm.

TPR analysis was done by feeding 40 mL/min of a 10 vol% H_2/N_2 mixture on a bench scale apparatus, by heating the material at 10 °C/min up to 800 °C. The product gas was analyzed with a Thermal Conductivity Detector after entrapping the possibly formed water through a condenser.

DLS and z−potential measurements were carried out using a Malvern Zetasizer Nano ZS instrument (Alfatest, Cinisello Balsamo, Milan, Italy), operating with a solid state He−Ne laser (wavelength source = 633 nm) at a working scattering angle of 173°, at 289 K on P25 and FSP samples suspended in bi-distilled water in various pH (3.5, 6.8 and 11) by using HCl and NaOH (Sigma Aldrich − Merck Life Science S.r.l., Milan, Italy) solutions for pH adjustment, in order to study the electrical charge density and the size distribution profile of the particles in solution.

3.3. Photoreactor and Testing Condition

The reactions were performed in a cylindrical photoreactor with a total volume of ca. 300 mL (holding 250 mL of solution) and equipped with a cooling jacket (Figure 7). A coaxial cylindrical submerged lamp was used as irradiation source, and a medium-pressure Hg vapor lamp (200 W UVA; Jelosil HG 200 L, Vimercate, Milan, Italy) with maximum emission at 365 nm was selected. The lamp power test was performed in the middle of the bulb using a photoradiometer (delta OHM HD2102,2; Jelosil, Vimercate, Milan, Italy), and it shows an average power of 60 W/m^2.

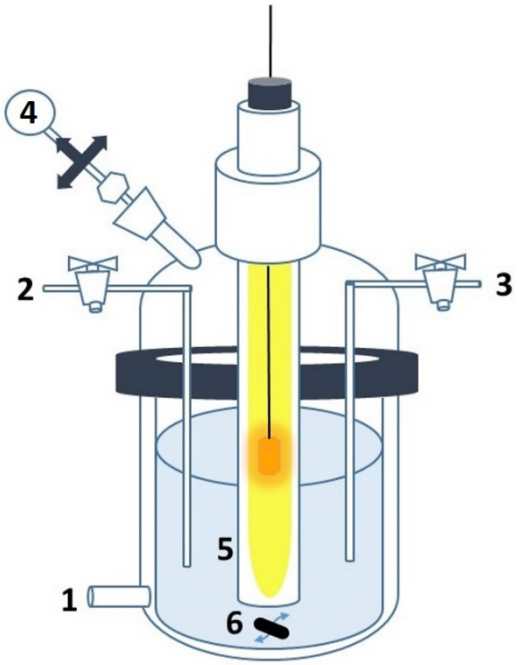

Figure 7. Sketch of the experimental photoreactor. (1) Water cooling system; (2) out gassing/gas feeding line; (3) liquid sampling; (4) gas sampling and line to gas chromatograph; (5) quartz shelter; (6) magnetic stirring.

The reactor included a degassing/air feeding inlet line (flow rate: 100 mL/min), which was used to continuously feed a mixture of He and O_2 (80:20 v/v) during testing in semibatch mode. In addition, two outlets were present, one for liquid phase sampling and a second one for gas output, which was directly connected to a gas chromatograph (HP 5890 Series II, Santa Clara, CA, USA).

An ammonia trap was placed on the gas line between the outlet of the reactor and the GC [47]. The double aim was to quantify stripped ammonia and to protect the GC from possible ammonia slip. The trap was tested in two forms. First, we placed a chemical trap as a drechsel bottle containing a diluted solution of H_2SO_4 (Sigma Aldrich−Merck Life Science S.r.l., Milan, Italy) in water (0.1 M), through which the gas flowing through the reactor was continuously flowing. The solution was periodically titrated using bromochresol green (Sigma Aldrich − Merck Life Science S.r.l., Milan, Italy) as an indicator, and negligible ammonia stripping was revealed under the selected reaction conditions (even at basic pH). This solution was not optimal for protecting the GC, since humidity accumulated progressively in the gas line, thus the drechsel for absorption in liquid phase was substituted with a solid adsorbent bed, filled with a dry acid zeolite (calcined at 550 °C for preactivation). The size was optimized in order to avoid excessive pressure drop through the outflowing line, thus avoiding the need of pressurization of the inlet flow. After use, the zeolite was discharged and analyzed through Thermo−Gravimetric Analysis to determine the weight loss. Periodic regeneration of the adsorbent was performed by heating to 300 °C to remove adsorbed water.

To better quantify the extent of possible stripping, we calculated the flash concentration of ammonia under worse basic conditions. The calculation was performed using the software Aspen Plus® (Aspentech Inc.) and by setting up a flash block. Operating at 25 °C, pH < 9, the stripping was negligible. At pH > 9, the calculated loss of ammonia reaching the gas phase was 2.1% (in mass); assuming a raise in temperature according to the maximum value ever reached in our tests (not with the presently used lamp), the maximum stripping calculated would be 4% (in mass, at 40 °C).

For each experiment, the reactor was loaded with a suspension of 250 mL of a 0.2 M NH_4Cl and 250 mg of catalyst (1 g/L), which was kept suspended by magnetic stirring.

After switching on the lamp, sampling of both the liquid and the gas phases was carried out every hour for a total reaction time of 5 h.

In addition, two blank tests were performed at pH 11.5, namely (a) pH 11.5, 0.2 M NH_4Cl without the catalyst under irradiation and (b) pH 11.5, 0.2 M NH_4Cl with catalyst in dark conditions; this was done to assess the role of homogeneous and non−photoinduced reactions or adsorption. Both blank experiments led to negligible observed conversion (ranging between −3.5 and +2.8%), further supporting the negligible stripping of ammonia, even under basic conditions, and suggesting broadly the error range.

An ion chromatograph (Metrohm, 883 Basic IC Plus, Origgio, VA, Italy) was used to quantify nitrite and nitrate ions concentration, while the indophenol standard method was used for the quantification of ammonia (and thus to calculate conversion) by UV−Vis spectroscopy (Perkin Elmer, Lambda 35, Milano, Italy). N_2 was analyzed by gas chromatography (HP 5890, Series II), which was connected online.

4. Conclusions

This work presents the performance of new catalysts prepared by flame spray pyrolysis (FSP). By operating at different pH, its optimal values resulted as 11.5 and 4.8 for P25 and FSP samples, respectively, considering a reasonable compromise between acceptable ammonia conversion and the reasonably low selectivity towards NO_3^- and NO_2^-.

The pH level may affect the adsorption on the surface of the catalysts, inducing an electrostatic interaction between charged reactants/intermediates and the charged surface. In this way, it may change the initial rates and consequently favor different reactions pathways, but this is not considered the rate determining step here. Indeed, pH values favoring the adsorption of NH_4^+ over a negatively charged surface were not univocally characterized by the highest conversion or reaction rate. On the contrary, basic pH induced an increase of the reaction rate favoring the production of strongly oxidizing radicals. This allowed not only for boosting the conversion but also the selectivity towards overoxidation products. Indeed, for both types of photocatalysts (P25 and FSP), conversion and selectivity were highly dependent on pH. At pH $\geq$ 9, the photooxidation of NH_3/NH_4^+ was effective, but this resulted in the nonnegligible formation of $NO_3^-$and NO_2^-, whereas, at more acidic pH, the selectivity to N_2 was satisfactory.

Finally, the addition of small amounts of metal co-catalysts (Ag, Au, Pt, Pd) to P25 at pH 11.5 notably increased the selectivity to nitrite and nitrate anions without significant improvement of ammonia conversion. By contrast, with FSP, tested at pH 4.8 (where lower conversion but higher selectivity is achieved), the addition of Au as co-catalysts was an effective strategy to increase the conversion, while a satisfactory selectivity toward N_2 was kept.

Supplementary Materials: The following are available online at https://www.mdpi.com/2073-4344/11/2/209/s1, Figure S1: N_2 adsorption/desorption isotherms collected at 77 K on P25 (full squares) and FSP (hollow triangles) outgassed overnight at 150°C., Figure S2: DR UV-Vis spectra of selected samples (a) and corresponding Tauc plots (b), Table S1: Physical−chemical data or the tested sample taken from [1].

Author Contributions: Conceptualization, I.R.; Data curation, A.T.; Funding acquisition, G.R. and I.R.; Investigation, E.B. and F.C.; Methodology, A.T.; Project administration, I.R.; Writing—original draft, E.B.; Writing—review & editing, I.R. and G.R. All authors have read and agreed to the published version of the manuscript.

Funding: This research was funded by Fondazione Cariplo, grant number 2015-0186.

Data Availability Statement: All the data relative to this research are reported in this manuscript and in the Supplementary Information file.

Acknowledgments: The financial support of Fondazione Cariplo through the measure "Ricerca sull'inquinamento dell'acqua e per una corretta gestione idrica", grant no. 2015-0186, is gratefully acknowledged.

Conflicts of Interest: The authors declare no conflict of interest.

References

1. Delwiche, C.C. *Denitrification, Nitrification, and Atmosphere Nitrous Oxide*; John Wiley & Sons: New York, NY, USA, 1981; pp. 107–108, ISBN 10-0471048968.
2. Lee, J.; Park, H.; Choi, W. Selective Photocatalytic Oxidation of NH_3 to N_2 on Platinized TiO_2 in Water. *Environ. Sci. Technol.* **2002**, *36*, 5462–5468. [CrossRef] [PubMed]
3. Huang, J.; Kankanamge, N.R.; Chow, C.; Welsh, D.T.; Li, T.; Teasdale, P.R. Removing Ammonium from Water and Wastewater Using Cost-Effective Adsorbents: A Review. *J. Environ. Sci.* **2018**, *63*, 174–197. [CrossRef]
4. Yang, J.; Wang, F.; Lv, J.; Liu, Q.; Nan, F.; Liu, X.; Xu, L.; Xie, S.; Feng, J. Interactive Effects of Temperature and Nutrients on the Phytoplankton Community in an Urban River in China. *Environ. Monit. Assess.* **2019**, *191*. [CrossRef] [PubMed]
5. Stumm, W.; Morgan, J. Chemical Equilibria and Rates in Natural Waters. In *Aquatic Chemistry*; John Wiley & Sons: New York, NY, USA, 1996; pp. 120–129.
6. Chapman, D.; Kimstach, V. Selection of water quality variables. In *Water Quality Assessments—A Guide to Use of Biota, Sediments and Water in Environmental Monitoring*; Chapman, D., Ed.; WHO: Geneva, Switzerland, 1992.
7. Appl, M. The Haber–Bosch Process and the Development of Chemical Engineering. In *A Century of Chemical Engineering*; Plenum Press: New York, NY, USA, 1982; pp. 29–54. ISBN 978-0-306-40895-3.
8. Rossetti, I. Reactor Design, Modelling and Process Intensification for Ammonia Synthesis. In *Sustainable Ammonia Production, Series Green Energy and Technology*; Springer Nature Switzerland AG: Charm, Switzerland, 2020; pp. 17–48.
9. Christensen, M.H.; Harremoes, P. Nitrification and Denitrification in Wastewater Treatment. *Water Pollut. J.* **1978**, *2*, 391–414.
10. Focht, D.D.; Chang, A.C. Nitrification and Denitrification Processes Related to Wastewater Treatment. *Adv. Appl. Microbiol.* **1975**, *19*, 153–186.
11. Pressley, T.A.; Bishop, D.F.; Roan, S.G. Ammonia-Nitrogen Removal by Breakpoint Chlorination. *Environ. Sci. Technol.* **1972**, *6*, 622–628. [CrossRef]
12. Compagnoni, M.; Ramis, G.; Freyria, F.S.; Armandi, M.; Bonelli, B.; Rossetti, I. Photocatalytic Processes for the Abatement of N-Containing Pollutants from Waste Water. Part 1: Inorganic Pollutants. *J. Nanosci. Nanotechnol.* **2017**, *17*, 3632–3653. [CrossRef]
13. Freyria, F.S.; Armandi, M.; Compagnoni, M.; Ramis, G.; Rossetti, I.; Bonelli, B. Catalytic and Photocatalytic Processes for the Abatement of N-Containing Pollutants from Wastewater. Part 2: Organic Pollutants. *J. Nanosci. Nanotechnol.* **2017**, *17*, 3654–3672. [CrossRef]
14. Gopalarao, G.; Murty, K.S. Photosensitisation by Solids. Part II. Photosensitized Oxidation Ofammoniain Aqueous Solution with Titania as the Photosensitiser. *J. Indian Chem. Soc.* **1941**, *18*, 361–370.
15. Bravo, A.; Garcia, J.; Domenech, X.; Peral, J. Some Aspects of the Photocatalytic Oxidation Ofammoniumion by Titanium Dioxide. *J. Chem. Res.* **1993**, 376–377.
16. Ren, H.T.; Liang, Y.; Han, X.; Liu, Y.; Wu, S.H.; Bai, H.; Jia, S.Y. Photocatalytic Oxidation of Aqueous Ammonia by Ag_2O/TiO_2 (P25): New Insights into Selectivity and Contributions of Different Oxidative Species. *Appl. Surf. Sci.* **2020**, *504*. [CrossRef]
17. Wang, J.; Song, M.; Chen, B.; Wang, L.; Zhu, R. Effects of PH and H_2O_2 on Ammonia, Nitrite, and Nitrate Transformations during UV254nm Irradiation: Implications to Nitrogen Removal and Analysis. *Chemosphere* **2017**, *184*, 1003–1011. [CrossRef] [PubMed]
18. Nagaveni, K.; Sivalingam, G.; Hegde, M.S.; Madras, G. Solar Photocatalytic Degradation of Dyes: High Activity of Combustion Synthesized Nano TiO_2. *Appl. Catal. B Environ.* **2004**, *48*, 83–93. [CrossRef]
19. Low, G.K.C.; McEvoy, S.R.; Matthews, R.W. Formation of Nitrate and Ammonium Ions in Titanium Dioxide Mediated Photocatalytic Degradation of Organic Compounds Containing Nitrogen Atoms. *Environ. Sci. Technol.* **1991**, *25*, 460–467. [CrossRef]
20. Pollema, C.H.; Milosavljevic, E.B.; Hendrix, J.L.; Solujic, L.; Nelson, J.H. Photocatalytic Oxidation of Aqueous Ammonia (Ammonium Ion) to Nitrite or Nitrate at TiO_2 Particles. *Monatsh. Chem.* **1992**, *123*, 333–339. [CrossRef]
21. Bonsen, M.; Schroeter, S.; Jacobs, H.; Broekaert, J.A.C. Photocatalytic Degradation of Ammonia with TiO_2 as Photocatalyst in the Laboratory and under the Use of Solar Radiation. *Chemosphere* **1997**, *35*, 1431–1445. [CrossRef]
22. Biyoghe Bi Ndong, L.; Ibondou, M.P.; Gu, X.; Lu, S.; Qiu, Z.; Sui, Q.; Maurice Mbadinga, S. Enhanced Photocatalytic Activity of TiO_2 Nanosheets by Doping with Cu for Chlorinated Solvent Pollutants Degradation. *Ind. Eng. Chem. Res.* **2014**, *53*, 1368–1376. [CrossRef]
23. Kumaresan, L.; Mahalakshmi, M.; Palanichamy, M.; Murugesan, V. Synthesis, Characterization, and Photocatalytic Activity of Sr^{2+} Doped TiO_2 Nanoplates. *Ind. Eng. Chem. Res.* **2010**, *49*, 1480–1485. [CrossRef]
24. Bahadori, E.; Compagnoni, M.; Tripodi, A.; Freyria, F.; Armandi, M.; Bonelli, B.; Ramis, G.; Rossetti, I. Photoreduction of Nitrates from Waste and Drinking Water. *Mater. Today Proc.* **2018**, *5*, 17404–17413. [CrossRef]
25. Bahadori, E.; Tripodi, A.; Ramis, G.; Rossetti, I. Semi-Batch Photocatalytic Reduction of Nitrates: Role of Process Conditions and Co-Catalysts. *ChemCatChem* **2019**, *11*, 4642–4652. [CrossRef]
26. Rossetti, I.; Biffi, C.; Bianchi, C.L.; Nichele, V.; Signoretto, M.; Menegazzo, F.; Finocchio, E.; Ramis, G.; Di Michele, A. Ni/SiO_2 and Ni/ZrO_2 Catalysts for the Steam Reforming of Ethanol. *Appl. Catal. B Environ.* **2012**, *117–118*, 384–396. [CrossRef]
27. Finocchio, E.; Rossetti, I.; Ramis, G. Redox Properties of Co- and Cu-Based Catalysts for the Steam Reforming of Ethanol. *Int. J. Hydrogen Energy* **2013**, *38*, 3213–3225. [CrossRef]

28. Compagnoni, M.; Lasso, J.; Di Michele, A.; Rossetti, I. Flame-Pyrolysis-Prepared Catalysts for the Steam Reforming of Ethanol. *Catal. Sci. Technol.* **2016**, *6*, 6257. [CrossRef]
29. Chiarello, G.L.; Rossetti, I.; Lopinto, P.; Migliavacca, G.; Forni, L. Preparation by Flame Spray Pyrolysis of $ABO_3 \pm \delta$ Catalysts for the Flameless Combustion of Methane. *Catal. Today* **2006**, *117*, 549–553. [CrossRef]
30. Zhu, X.; Castleberry, S.R.; Nanny, M.A.; Butler, E.C. Effect of PH on the Photocatalytic Oxidation of Aqueous Ammonia and Nitrite in Titanium Dioxide Suspensions. *Environ. Sci. Technol.* **2005**, *39*, 3784–3791. [CrossRef] [PubMed]
31. Pagsberg, P.B. Investigation of the NH_2 Radical Produced by Pulse Radiolysis of Ammonia in Aqueous Solution. *Ris. Rep.* **1972**, *256*, 209–221.
32. Neta, P.; Maruthamuthu, P.; Carton, P.M.; Fessenden, R.W. Formation and Reactivity of the Amino Radical. *J. Phys. Chem.* **1978**, *82*, 1875–1878. [CrossRef]
33. Milis, A.; Doménech, X. Photoassisted Oxidation of Nitrite and Nitrate over Different Semiconducting Oxides. *J. Photochem. Photobiol. A Chem.* **1993**, *72*, 55–59. [CrossRef]
34. Letterman, R.D.W. Quality and treatment: A handbook of community water supplies. In *American Water Works Association*; McGraw-Hill: New York, NY, USA, 1999; Chapter 6.
35. Shibuya, S.; Sekine, Y.; Mikami, I. Influence of PH and PH Adjustment Conditions on Photocatalytic Oxidation of Aqueous Ammonia under Airflow over Pt-Loaded TiO_2. *Appl. Catal. A Gen.* **2015**, *496*, 73–78. [CrossRef]
36. Ogata, Y.; Tomizawa, K.; Adachi, K. Photooxidation of Ammonia with Aqueous Hydrogen Peroxide. *Mem. Fac. Eng. Nagoya Univ.* **1981**, *3*, 58–65.
37. Kuo, C.H.; Yuan, F.; Hill, D.O. Kinetics of Oxidation of Ammonia in Solutions Containing Ozone with or without Hydrogen Peroxide. *Ind. Eng. Chem. Res.* **1997**, *36*, 4108–4113. [CrossRef]
38. Huang, L.; Li, L.; Dong, W.; Liu, Y.; Hou, H. Removal of Ammonia by OH Radical in Aqueous Phase. *Environ. Sci. Technol.* **2008**, *42*, 8070–8075. [CrossRef]
39. Hoigne, J.; Bader, H. Ozonation of Water: Kinetics of Oxidation of Ammonia by Ozone and Hydroxyl Radicals. *Environ. Sci. Technol.* **1978**, *12*, 79–84. [CrossRef]
40. Wang, A.; Edwards, J.G.; Davies, J.A. Photooxidation of Aqueous Ammonia with Titania-Based Heterogeneous Catalysts. *Sol. Energy* **1994**, *52*, 459–466. [CrossRef]
41. Altomare, M.; Chiarello, G.L.; Costa, A.; Guarino, M.; Selli, E. Photocatalytic Abatement of Ammonia in Nitrogen-Containing Effluents. *Chem. Eng. J.* **2012**, *191*, 394–401. [CrossRef]
42. Altomare, M.; Dozzi, M.V.; Chiarello, G.L.; Di Paola, A.; Palmisano, L.; Selli, E. High Activity of Brookite TiO_2 Nanoparticles in the Photocatalytic Abatement of Ammonia in Water. *Catal. Today* **2015**, *252*, 184–189. [CrossRef]
43. Li, A.; Wang, Z.; Yin, H.; Wang, S.; Yan, P.; Huang, B.; Wang, X.; Li, R.; Zong, X.; Han, H.; et al. Understanding the Anatase-Rutile Phase Junction in Charge Separation and Transfer in a TiO_2 Electrode for Photoelectrochemical Water Splitting. *Chem. Sci.* **2016**, *7*, 6076–6082. [CrossRef] [PubMed]
44. Nakajima, H.; Mori, T.; Shen, Q.; Toyoda, T. Photoluminescence Study of Mixtures of Anatase and Rutile TiO_2 Nanoparticles: Influence of Charge Transfer between the Nanoparticles on Their Photoluminescence Excitation Bands. *Chem. Phys. Lett.* **2005**, *409*, 81–84. [CrossRef]
45. Altomare, M.; Selli, E. Effects of Metal Nanoparticles Deposition on the Photocatalytic Oxidation of Ammonia in TiO_2 Aqueous Suspensions. *Catal. Today* **2013**, *209*, 127–133. [CrossRef]
46. Chiarello, G.L.; Rossetti, I.; Forni, L. Flame-Spray Pyrolysis Preparation of Perovskites for Methane Catalytic Combustion. *J. Catal.* **2005**, *236*, 251–261. [CrossRef]
47. Rossetti, I.; Compagnoni, M.; Ramis, G.; Freyria, F.; Armandi, M.; Bonelli, B. Development of Unconventional Photocatalytic Reactors and Processes for the Abatement of Harmful N-Containing Pollutants. *Chem. Eng. Trans.* **2017**, *57*, 1663. [CrossRef]